

## Cell-Based Gene Therapy for Repair of Critical Size Defects in the Rat Fibula

ZaWaunyka W. Lazard,<sup>1</sup> Michael H. Heggeness,<sup>2</sup> John A. Hipp,<sup>2</sup> Corinne Sonnet,<sup>1</sup> Angie S. Fuentes,<sup>2</sup> Rita P. Nistal,<sup>1</sup> Alan R. Davis,<sup>1,2,3</sup> Ronke M. Olabisi,<sup>4</sup> Jennifer L. West,<sup>1,4</sup> and Elizabeth A. Olmsted-Davis<sup>1,2,3\*</sup>

<sup>1</sup>Center for Cell and Gene Therapy, Baylor College of Medicine, Houston, Texas 77030

<sup>2</sup>Department of Orthopedic Surgery, Baylor College of Medicine, Houston, Texas 77030

<sup>3</sup>Department of Pediatrics–Hematology Oncology, Baylor College of Medicine, Houston, Texas 77030

<sup>4</sup>Department of Bioengineering, Rice University, 6500 Main St. MS 142, Houston, Texas 77030

### ABSTRACT

More than a decade has passed since the first experiments using adenovirus-transduced cells expressing bone morphogenetic protein 2 were performed for the synthesis of bone. Since this time, the field of bone gene therapy has tackled many issues surrounding safety and efficacy of this type of strategy. We present studies examining the parameters of the timing of bone healing, and remodeling when heterotopic ossification (HO) is used for bone fracture repair using an adenovirus gene therapy approach. We use a rat fibula defect, which surprisingly does not heal even when a simple fracture is introduced. In this model, the bone quickly resorbs most likely due to the non-weight bearing nature of this bone in rodents. Using our gene therapy system robust HO can be introduced at the targeted location of the defect resulting in bone repair. The HO and resultant bone healing appeared to be dose dependent, based on the number of AdBMP2-transduced cells delivered. Interestingly, the HO undergoes substantial remodeling, and assumes the size and shape of the missing segment of bone. However, in some instances we observed some additional bone associated with the repair, signifying that perhaps the forces on the newly forming bone are inadequate to dictate shape. In all cases, the HO appeared to fuse into the adjacent long bone. The data collectively indicates that the use of BMP2 gene therapy strategies may vary depending on the location and nature of the defect. Therefore, additional parameters should be considered when implementing such strategies. *J. Cell. Biochem.* 112: 1563–1571, 2011. © 2011 Wiley-Liss, Inc.

**KEY WORDS:** HETEROTOPIC OSSIFICATION; CRITICAL SIZE DEFECT; BONE REPAIR

Successful bone repair of non-unions remains a complex challenge in orthopedics today. Segmental bone loss resulting from trauma, cancer progression and various bone diseases are treated with bone grafting procedures that occur approximately 500,000 times annually in the United States [Laurencin et al., 2006]. Around 11% of the non-fatal injuries in the United States involve long bone fractures [Vyrostek et al., 2004] and on average non-union rates occur in about 10% of these cases, varying with the intervention treatment and type of long bone involved [Giannoudis and Atkins, 2007; Tzioupis and Giannoudis, 2007]. All of these factors contribute to a significant toll on the patients, through lengthy recovery times, changes in quality of life, and enormous expense associated with the course of treatment.

Bone distraction osteogenesis, free vascularized bone transfer, limb shortening, and autologous bone grafts are common methods used to manage post-traumatic segmental bone defects in any of the long bone segments. Specific conditions like mechanical instability, axial deviation, bone defect size, and presence of infection must be addressed with the treatment being customized to each specific case. Distraction osteogenesis, with either the lengthening or bone transport technique, uses the Ilizarov apparatus to stabilize the limb and treat very large defects, up to 30 cm. However, this procedure is plagued with long treatment duration and numerous complications including delayed union at the docking site and devascularization of the transport segment [DeCoster et al., 1999]. The complication rate (major and minor) associated with the Ilizarov technique has been

Grant sponsor: DAMD; Grant number: W81XWH-07-1-0215; Grant sponsor: DARPA; Grant number: W911NF-09-1-0040.

\*Correspondence to: Dr. Elizabeth Olmsted-Davis, PhD, One Baylor Plaza Alkek N1010, Houston, TX 77030.  
E-mail: edavis@bcm.edu

Received 2 February 2011; Accepted 4 February 2011 • DOI 10.1002/jcb.23068 • © 2011 Wiley-Liss, Inc.  
Published online 22 February 2011 in Wiley Online Library (wileyonlinelibrary.com).

reported to reach as high as 87% [Motsitsi, 2008]. Vascularized bone transplantation can be performed with iliac crest, fibula, or rib but it has significant drawbacks involving donor site morbidity and increased fracture risk [DeCoster et al., 2004]. Limb shortening is restricted to bone defects less than 3 cm and has the shortest treatment time, but it is also associated with excessive soft tissue swelling and loss of limb function [Watson et al., 1995].

Today the gold standard of care for segmental bone loss has become autologous bone graft, but it is limited by graft material availability. Therapies are also plagued with a plethora of complications and drawbacks. Infection, implant failure, dysfunctional limb, unplanned additional surgical procedure, high cost, and prolonged treatment time are only a few of the shortcomings associated with these treatments [Finkemeier, 2002; DeCoster et al., 2004; Sen and Miclau, 2007]. A 30% failure rate is associated with the surgical treatments for segmental bone defects [Sorger et al., 2001].

Bone graft materials are selected based on their osteogenic, osteoinductive, and osteoconductive qualities that would produce the best healing and mechanical stability for each individual case. Osteoinduction refers to the ability of the material to stimulate the host precursor cells to form new bone through their differentiation into chondroblasts or osteoblasts. The osteoinductive capacity of a graft depends on the amount and type of growth factors and cytokines present.

One of the most promising growth factors currently being tested is bone morphogenetic protein 2 (BMP2), which can induce both orthotopic and de novo bone formation at targeted locations. Recombinant human rhBMP-2 and rhBMP-7 are approved for clinical application and are commercially available, although neither has been determined to be efficacious in long bone repair by the FDA. One problem associated with the use of the recombinant proteins, beyond the expense and extremely high amount that must be delivered for any effect, is their extremely short half lives in vivo at approximately 24 h [Winn et al., 2000; Jeon et al., 2007]. Further, because of their short retention at the target site additional carrier materials must be implanted as well, thus increasing the risk of infection and making placement of the material difficult [Hollinger et al., 1998; Haidar et al., 2009].

Many have attempted to deliver the BMP2 through gene therapy means in order to overcome delivery of protein that has limited efficacy. These approaches employ either retroviral-transduced cells or the direct use of adenovirus with both methods having serious limitations. The delivery of retroviral-transduced cells, which carry 1–2 copies of the BMP2 gene, provide low levels of the protein locally and allow for these genetically modified cells expressing BMP2 to be incorporated into the bone which increases the overall risk of unwanted long-term adverse reactions [Moutsatsos et al., 2001]. Researchers have also attempted to introduce non-integrating vectors, such as adenovirus or adeno-associated virus [Lieberman et al., 1998; Gafni et al., 2004], directly into the animal which has a large number of associated problems, including poor transduction efficiencies [Olmsted et al., 2001] and diffusion of the free virus expressing BMP2 to other tissues such as the liver and lungs [Baltzer et al., 2000; Gelse et al., 2001]. The injection of the free virus results in limited to no efficacy along with undetectable

amounts of protein being expressed at the desired site, as well as significant risk to other tissues such as the liver.

To circumvent these problems we have employed a cell-based gene therapy approach, which eliminates the use of free virus in the organism and ensures reliable, efficient transduction, and/or expression of the BMP2 at the target site. Further, the BMP2 transgene cannot integrate into the chromosome, and with the use of a first generation vector the transduced cells are rapidly cleared by the immune system [Fouletier-Dilling et al., 2007]. Again, because the cells are transduced *ex vivo*, with a replication defective adenovirus, the resultant cells are not considered to be infectious or contain any infectious material, thus there is minimal risk associated with the use of this gene therapy system. Additionally, this system provides a sufficient local concentration of the BMP2 at the target site but the transgene does not integrate into the chromosome, so there is no long-term risk associated with chronic BMP2 expression, or other gene disruption from the insertion. Finally, in our previous studies of heterotopic ossification (HO), we have determined that the cells do not incorporate into the final bone structures and are only acting to deliver the BMP2. This importantly avoids potential long-term adverse reactions arising from the inclusion of the foreign materials in the skeletal bone.

In the studies presented here, we are harnessing the bone induction capability of recombinant adenoviral-transduced cells to safely and efficaciously deliver BMP2. This cell-based gene therapy system provides sufficient BMP2 protein in vivo at a specific targeted location to induce rapid repair of a critical size defect introduced into the rat fibula. This circumvents the need for releasing carriers and supraphysiological concentrations of BMP2. Furthermore, the rat fibula model is somewhat unique in that it is fused at the ends to the adjacent tibia, thus creating a non-weight bearing environment. We have noted that even a simple fracture introduced into the fibula does not heal, but rather undergoes extensive resorption leaving an approximate 10 mm size defect. Thus, repair of this bone would represent an extremely challenging environment. In the studies presented here, we demonstrate the parameters required by this system for bone healing and find that complete healing occurred by 6 weeks in 100% of the animals. Further, we followed the animals for an additional 6 weeks beyond this point to confirm that the fibula was stable and no additional changes resulted post-healing.

## MATERIALS AND METHODS

### CELL CULTURE

A human fibroblast cell line (MRC5) was acquired from the American Type Culture Collection (Manassas, VA) and propagated in Dulbecco's modified Eagle's medium (DMEM). The medium was supplemented with 10% fetal bovine serum (FBS; Hyclone, Logan, UT), penicillin (100 U/ml), streptomycin (100 µg/ml), amphotericin B (0.25 µg/ml; Invitrogen Life Technologies, Gaithersburg, MD), and tetracycline (3 mg/L; Sigma, St. Louis, MO). MRC5 cells are not capable of inducing bone formation before transduction.

W20-17, a murine stromal cell line, was obtained as a gift from Genetic Institute (Cambridge, MA) and was propagated as described by Thies et al. [1992]. The W20-17 cells were briefly grown in

supplemented DMEM and cultured at a subconfluent density in order to maintain the phenotype. All cell types were grown at 37°C and 5% CO<sub>2</sub> in humidified air.

### ADENOVIRUS TRANSDUCTION

A replication-defective E1- to E3-deleted human adenovirus type 35 fiber protein (Ad5F35) were constructed to contain cDNAs for BMP2 in the E1 region of the virus [Olmsted-Davis et al., 2002] or did not contain any transgene in this region, AdEmpty. The resultant purified viruses, AdBMP2, and AdEmpty cassette, had viral particle (VP)-to-plaque-forming unit (PFU) ratios of 1:77 and 1:111, respectively, and all viruses were confirmed to be negative for replication-competent adenovirus [Olmsted-Davis et al., 2002]. Cells were transduced as previously described with AdBMP2 or AdEmpty cassette at a viral concentration of 2,500 VP/cell [Olmsted-Davis et al., 2002; Fouletier-Dilling et al., 2007]. MRC5 cells were transduced with either AdEmpty or AdBMP2 in DMEM supplemented with 2% FBS at a concentration of 2,500 VP/cell. Adenovirus was allowed to incubate overnight at 37°C, humidified atmosphere, 5% CO<sub>2</sub>.

### QUANTIFICATION OF BMP2

BMP2 protein was measured in culture supernatant taken from cells 72 h after transduction with AdBMP2 and culture supernatant was collected and assayed for BMP2 protein using a Quantikine BMP2 immunoassay ELISA kit (DBP200; R&D Systems, Minneapolis, MN). BMP2 protein activity was quantified in culture supernatant collected from cells after transduction with AdBMP2 or AdEmpty cassette or no virus, and a portion incubated with W20-17 bone marrow stromal cells, which rapidly increases alkaline phosphatase expression. Alkaline phosphatase activity is readily quantified [Blum et al., 2001]. Briefly, W20-17 cells were plated in 24-well plates at subconfluent densities ( $5 \times 10^4$  cells/cm<sup>2</sup>) and 24 h later the media was replaced with 200  $\mu$ l of fresh media and 200  $\mu$ l of conditioned culture media from various cells doses. W20-17 cells were then assayed for alkaline phosphatase activity 72 h after the addition of conditioned culture supernatant using a chemiluminescence procedure [Olmsted et al., 2001]. Cellular alkaline phosphatase was extracted by washing the cells with PBS and cells were lysed with three cycles of freeze thaw in 100  $\mu$ l/cm<sup>2</sup> of 25 mM Tris-HCl, pH 8.0, and Triton X-100. For detection of alkaline phosphatase 2  $\mu$ l of CSPD<sup>®</sup> ready-to-use with Sapphire II enhancer (Tropix, Bedford, MA) in an eppendorf tube, vortexed, and incubated at room temperature for 30 s. The light output from each sample was integrated for 10 s after a 2-s delay by a Glomax 20/20 luminometer (Promega, Madison, WI). Alkaline phosphatase detection signal was recorded in relative luminescence units (RLU).

### CRITICAL SIZE DEFECT MODEL

The critical size defect was introduced into the rat fibula. Adult homozygous Athymic RNU Nude rats weighing (200–300 g) were administered buprenorphine at 0.5 mg/kg by subcutaneous injection into the right thigh 1 h prior to surgery. The rats underwent general anesthesia through the use of an animal vaporizer that dispensed isoflurane at 2–4% initial induction and 1–2% throughout the surgery. Each animal was shaved, disinfected with Hibiclens and

isolated to a sterile surgical field that included a surgical drape that allowed only the left hind limb to be exposed. A lateral incision in the skin of about 2 cm was performed on the lower leg, along with a smaller incision into the gastrocnemius muscle. This muscle was retracted in order to expose the fibula and an osteotomy was performed to create a 2–4 mm segmental defect on the diaphysis of the fibula. Cells were then introduced into the defect void by placement into a sutured muscle pocket. Animals (n = 8) were euthanized and tissues isolated at various time points as indicated in the text. All animal studies were performed in accordance with the standards of Baylor College of Medicine, Department of Comparative Medicine, after review and approval of the protocol by the Institutional Animal Care and Use Committee (IACUC).

### RADIOGRAPHIC ANALYSIS OF THE NEW BONE

Hind limbs were harvested and radiographically analyzed using an XPERT model faxitron (Kubtec, Fairfield, CT) in biplanar projections. Samples were set at an exposure time of 15 s and acceleration voltage of 30 kV. Bone healing was evaluated with radiographs at the termination of each study.

Qualitative radiographic analyses were performed using micro-computed tomography (MicroCT) system (eXplore Locus SP; GE Healthcare, London, ON, Canada) at 14  $\mu$ m resolution. Bone density was determined with a density calibration phantom. Three-dimensional reconstructions and cross-sections of the hind limb were generated to identify the defect void and new bone.

### HISTOLOGICAL ANALYSIS OF THE NEW BONE

Animals (n = 8) were euthanized at weekly intervals starting at 2 weeks and ending at 12 weeks. Hind limbs were isolated; formalin fixed, and decalcified paraffin embedded. Serial sections (5  $\mu$ m) were prepared that encompassed the critical defect site. Hematoxylin and eosin staining was performed on every fifth slide to locate the newly forming endochondral bone. All sections were analyzed by light microscopy.

## RESULTS

### MODEL OF CRITICAL SIZE DEFECT

Varying sizes of bone were removed from the rat fibula starting with a simple fracture (1 mm), and systematically increasing in 1 mm increments to a maximum of 10 mm. The rat fibula was selected over other potential bones because unlike in humans, in rodents this bone is uniquely fused to the adjacent tibia. Therefore, a critical defect can readily be introduced without need for additional fixation. After 2 weeks bone healing was radiologically evaluated using micro-computational tomography ( $\mu$ CT). Surprisingly, in all cases 1, 2, 5, and 10 mm defects (Fig. 1A–D, respectively) we observed a similar size defect of approximately 10 mm or the maximum size introduced into the bone, and the bone ends appeared to be pointed, suggesting that the bone was undergoing significant resorption. Rotation of the  $\mu$ CT images indicated that the bone ends were healed with no apparent sign of an open bone marrow cavity. This indicates that in all cases the bone was not only unable to repair, but that it no longer could maintain normal bone remodeling and had initiated

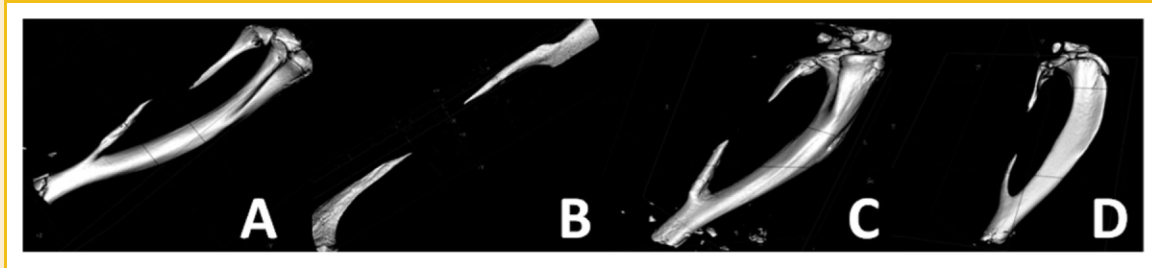


Fig. 1. Representative three-dimensional reconstructions of rat fibulas through microcomputational analysis. Varying sizes of defects (1–10 mm) were surgically introduced into rat fibulas and 2 weeks later analyzed for the presence of bone repair. The results depicted show an approximately 10 mm defect independent of the original defect size (A) 1 mm, (B) 2 mm, (C) 5 mm, and (D) 10 mm.

resorption. These results imply that any defect introduced into this model is a significant challenge for bone repair.

#### DOSE RESPONSE TO ADBMP2-TRANSDUCE CELLS

We next defined the dose of AdBMP2-transduced cells required to provide optimal healing of the bone defect. Fibroblasts were transduced with AdBMP2 at 2,500 vp/cell [Gugala et al., 2003] and BMP2 protein as well as activity was quantified 72 h later. Total BMP2 protein within the culture supernatant was approximately 18.6 ng per  $1 \times 10^6$  cells (Fig. 2A). Cells transduced with AdEmpty, as well as untransduced cells, did not produce BMP2. Interestingly, a standard dose of recombinant BMP2 protein used to induce bone formation in a rat critical size defect was approximately 12  $\mu$ g [Endo et al., 2006]. Since  $5 \times 10^6$  BMP2-producing cells is adequate to heal the bone completely (Fig. 3A), and we have determined that the transduced cells are present at a maximum of 5 days

[Fouletier-Dilling et al., 2007]. This means that a maximum of 93 ng is sufficient to completely heal the bone in this model. This is 130 times less than the amount of protein used in other rat defect studies with recombinant BMP2 suggesting that the prolonged local generation of BMP2 is critical to success due to the short half life of the protein [Endo et al., 2006].

Further, BMP2 protein activity, as determined by the elevation in the BMP2 responsive protein alkaline phosphatase [Blum et al., 2001], showed that this BMP2 being made is active (Fig. 2B). At no time did we observe either BMP2 activity or protein in culture supernatant isolated from the AdEmpty cassette cells or cells alone. Various numbers of the AdBMP2-transduced cells were next injected simultaneously with the introduction of a 3 mm bone defect in the fibula. The cells were injected into the void region, and surrounding muscle tissues of the rats ( $n = 5$ ), and potential bone formation allowed to progress for 2 weeks. Representative images of

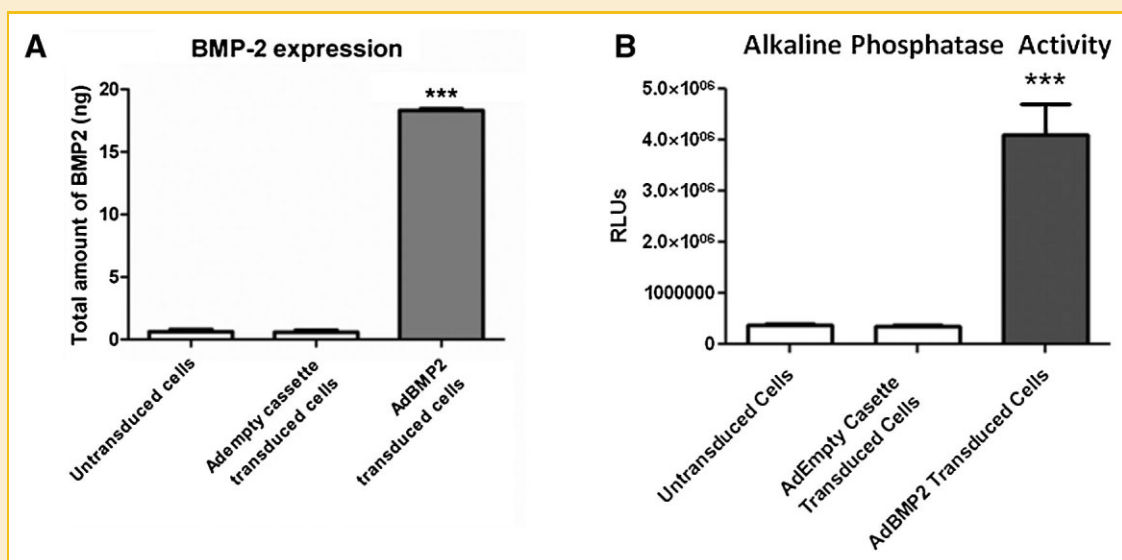


Fig. 2. Quantification of BMP2 protein and activity from adenovirus-transduced cells. A: BMP2 activity in culture supernatant collected 72 h after transduction with AdBMP2- or AdEmpty cassette-transduced cells (2,500 vp/cell) was quantified using an ELISA. BMP2 protein is represented as total protein produced by  $5 \times 10^6$  cells. Error bars represent means  $\pm$  SD for  $n = 5$ . A Student's *t*-test was applied to demonstrate significance. B: Alkaline phosphatase activity in W20-17 cells after addition of conditioned media from AdBMP2- or AdEmpty cassette-transduced cells (2,500 vp/cell). To demonstrate endogenous levels of alkaline phosphatase we included the cells alone. Alkaline phosphatase activity is depicted as the average relative chemiluminescence units (RLU), where  $n = 3$ . Error bars represent means  $\pm$  SD for  $n = 3$ . A Student's *t*-test was applied to demonstrate significance.

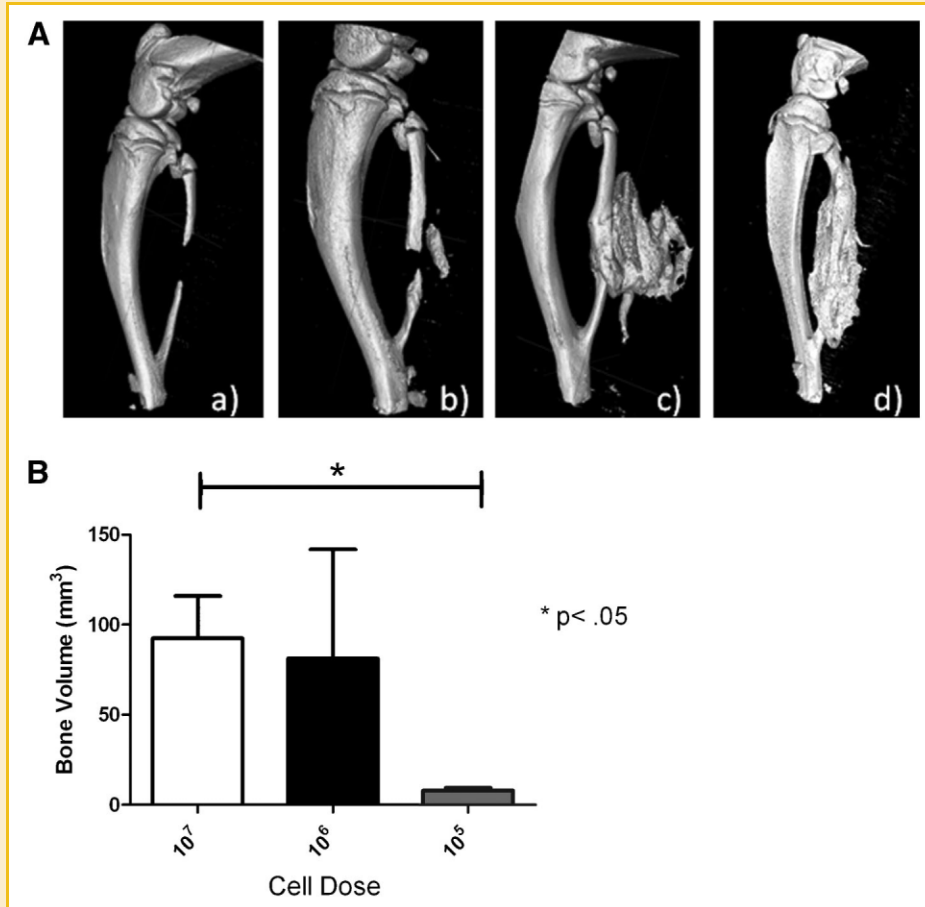


Fig. 3. Resultant bone formation from the introduction of adenovirus-transduced cells into the defect site. A: Representative three-dimensional surface renderings obtained from microcomputational analysis of the resultant bone repair 2 weeks after introduction of critical size defect in the rat fibula and delivery of varying numbers of AdBMP2-transduced cells; (a)  $5 \times 10^4$  cells, (b)  $5 \times 10^5$ , (c)  $5 \times 10^6$ , (d)  $5 \times 10^7$ . B: Quantification of the bone repair using microcomputational analysis. Bone volume of the newly forming bone as depicted in (A), was calculated for each cell dose ( $n = 5$  per group). The means and standard deviations for each group were calculated and compared using a one-way analysis of variance.

the resulting new bone are shown in Figure 3. As seen in Figure 3A, the new bone formation varied drastically with cell numbers. At no time did we observe bone formation or healing in the samples receiving  $5 \times 10^4$  cells, suggesting that there is a threshold amount of BMP2 required for inducing bone formation. Alternatively, there was no statistical difference between the two highest cell numbers or doses (Fig. 3B), indicating that there is a maximum bone formation response that can be achieved with this system. No bone formation was observed in with the  $5 \times 10^4$  cell dose, whereas there is a significant 10-fold change in bone volume between the  $5 \times 10^5$  and  $5 \times 10^7$  cell doses. There was a significant difference between the highest doses  $5 \times 10^6$  and  $5 \times 10^7$  suggesting that this may be a maximum response to BMP2. For that reason, we used this dose for all subsequent experiments.

#### BONE HEALING OF THE FIBULA DEFECT

We next determined the ability of the therapy to heal the critical size defect over 12 weeks. Figure 4 shows there is substantial bone formation at 2 weeks using this dose of cells, which appears to quickly resorb and by 4 weeks the new bone more closely resembles

the fibula that it is replacing. However, as seen in the cross-sectional  $\mu$ CT (Fig. 4F) new bone appears to be immature in nature. Although it spans the defect and is contiguous with the skeletal bone, it has not remodeled to have contiguous cortices, which suggests that this may not be well integrated at this stage. Alternatively, by 6–12 weeks a cortical bone structure begins to appear in the newly formed bone (Fig. 4H–J), suggesting that the bone is being remodeled and most likely fused. Bone healing and remodeling appears to be complete by 6 weeks (Fig. 4H) with little additional remodeling occurring at weeks 9–12. Interestingly, there appears to be additional bone attached to the skeletal bone (Fig. 4C–E), or actual residual HO that has not been resorbed. Additionally, some samples appeared to have a small amount of residual HO which was not attached to the fibula, but remained in the muscle between fibers.

We next looked at the bone architecture by analyzing cross-sectional cuts through the bone. The architecture appeared to change dramatically over the course of bone healing. Changes in bone architecture are a component of bone remodeling and aid in determining if the new bone has truly fused to the skeletal bone. Fusion at the defect site is a critical parameter in this system, because

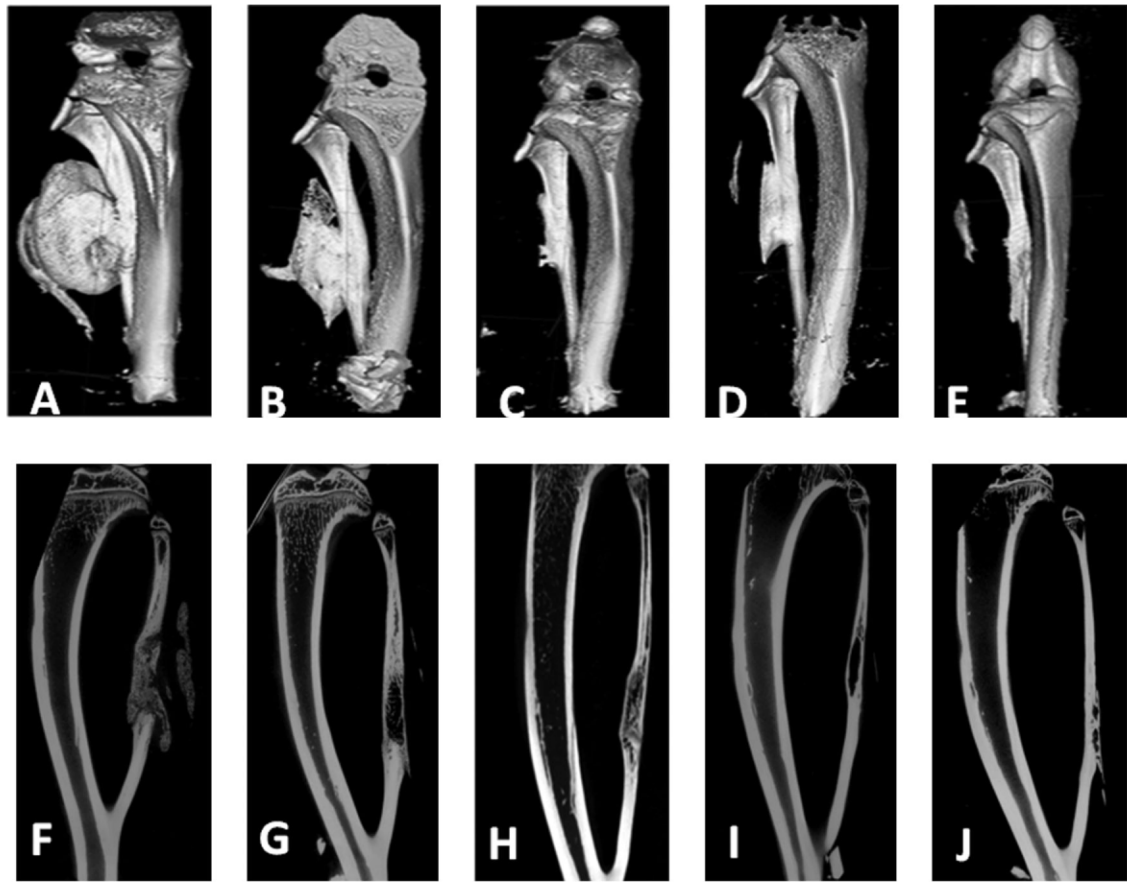


Fig. 4. Microcomputational analysis of bone healing over time. Representative three-dimensional surface renderings (A–E) or two-dimensional reconstructions (F–J) of bone healing over time; (A,F) 2 weeks; (B,G) 4 weeks; (C,H) 6 weeks; (D,I) 9 weeks; and (E,J) 12 weeks after introduction of the AdBMP2-transduced cells in the fibula defect;  $n = 9$  per group.

the majority of the new bone is made de novo, as HO, and it must fuse to the skeletal bone to complete healing. At 2 weeks the new bone is found throughout the skeletal defect (Fig. 4F); however, it appears to be immature bone, which has not remodeled or integrated into the adjacent skeletal bone. This is in contrast to the adjacent skeletal bone, which has well-defined cortices and a hollow bone marrow cavity. Thus, although there is new bone, it does not appear to be well fused into the skeletal bone, or healed to the point such that it is one contiguous remodeled structure. However, by 6 weeks portions of the new bone appear to be remodeled with defined cortical bone and the tentative fusion site are less apparent (Fig. 4H), suggesting that the bone is integrated and almost completely healed. By 9–12 weeks, we observed integrated structures with the only abnormality being the additional small amounts of bone on the outer cortex (Fig. 4I,J).

We next examined the bone healing through histological analysis to confirm the remodeling and fusion of the newly formed bone with the skeletal bone. This requires bone remodeling to replace the woven bone and lamellar bone junction with integrated remodeled bone. Photomicrographs from representative samples of the healing fibulas show substantial immature bone that completely fills and surrounds the defect (Fig. 5). Over time however, the bone remodels

considerably and new cartilage is no longer present in the tissues (Fig. 5B). By 6 weeks, the bone appears to be considerably more mature, with thicker cortical area that are contiguous with the skeletal cortical bone (Fig. 5C). Interestingly, the adjacent cortical bone appears to have a significant gap, which may represent either an area where the bone is vascularized, as evidenced by the pooling of blood or alternatively, a defect introduced during healing (Fig. 5C). However, this defect was not observed through radiograph analysis (Fig. 4C), suggesting that it comprises a relatively small region of the new bone. It is also of interest to note that in the serial sections where this cortex appears uniform and contiguous, the adjacent cortex now appears ruffled. This indicates that although it is healing, the new shape of the bone does not exactly mimic the original fibula. At 9 and 12 weeks, there is once more additional bone on the exterior of the fibula. However, the interior cortex appears uniform and similar to the normal fibula (Fig. 5D,E).

## DISCUSSION

These studies are the first to introduce a cell-based gene therapy system into a rat critical size defect model and have it lead to rapid

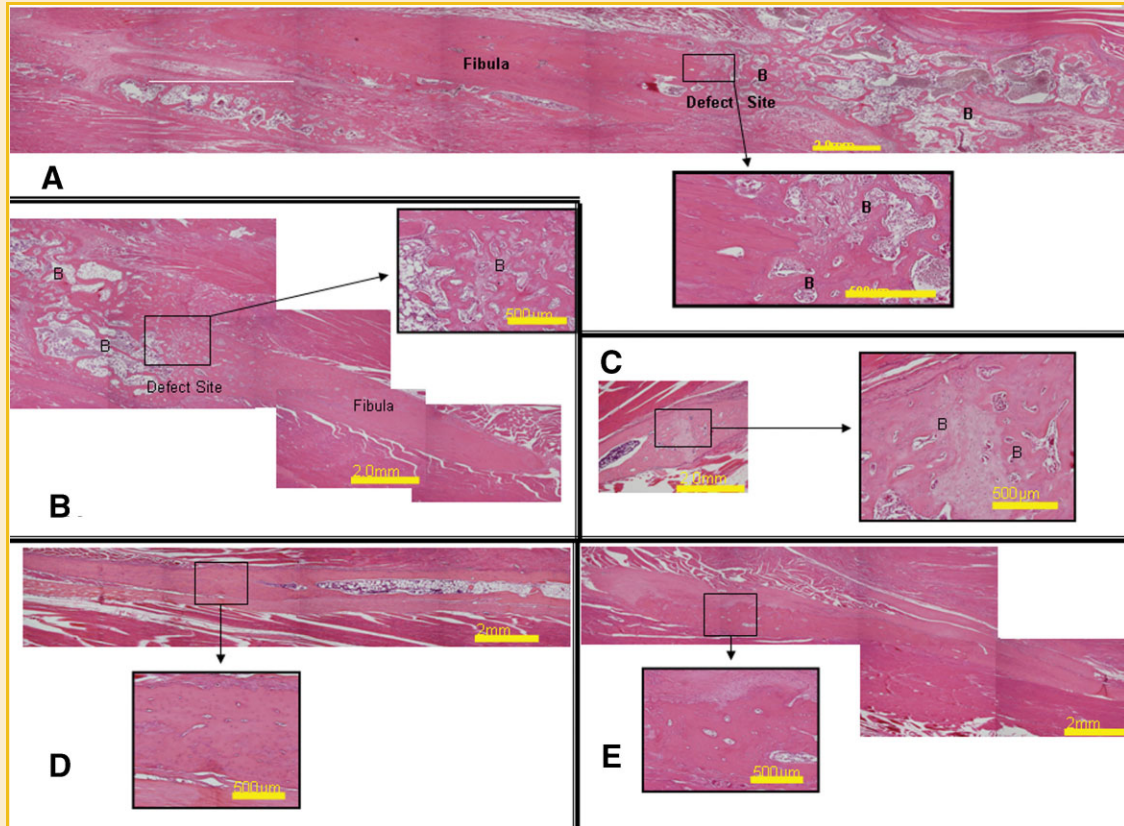


Fig. 5. Representative photomicrographs of the fibula defect at various times after introduction of the AdBMP2-transduced cells. Tissues were formalin fixed decalcified, paraffin embedded and serial sectioned ( $5\ \mu\text{m}$ ) through the entire fibula region. Every fifth section was hematoxylin and eosin stained, and images taken which were representative of the defect region in particular the junction with the fibula at various times, (A) 2 weeks, (B) 4 weeks, (C) 6 weeks, (D) 9 weeks, and (E) 12 weeks. The appearance of bone is identified with (B).

replacement and repair of the bone. HO can successfully be induced and directed to heal a critical size defect even in bone conditions that favor bone resorption. The HO, once touching the skeletal bone, can prevent rapid resorption and enhance the bone formation, remodeling, and fusion. The overall complete healing occurs rapidly from 2 to 6 weeks with 100% healing and repair completed by 6 weeks. Interestingly, little remodeling or additional resorption appears to occur after this time. In many cases after the initial resorption, there are small amounts of bone either heterotopic or orthotopic that are associated with the structures and appear to persist. This may be due in part to the non-weight bearing nature of this bone.

The rat fibula was selected for this model based on the unique fusion of this bone to the adjacent tibia. Thus, the tibia functions as an external support and no additional fixation is required, allowing this to be a very fast and reliable model. To our surprise, studies to determine the critical distance that would be unable to heal on its own showed even a simple fracture led to rapid resorption and non-union of this bone. Interestingly, since this bone is non-weight bearing in the rodent due to the fusion with the tibia, the rapid resorption may be a result from the lack of forces on this bone. Similar phenomenon has been reported in cases where HO has become extensive enough to become weight bearing, leading to the

almost complete resorption of the normal skeletal bone. Further, it has long been known that disuse of skeletal bone during immobilization can lead to elevated resorption. Therefore this model, beyond its versatility, becomes one of the most challenging of all bone repair models for the investigation of bone healing. With bone remodeling favoring resorption, contribution to new bone formation is challenging and thus may be even more difficult to obtain fusion and complete repair.

Complete bone healing could be reliably achieved using a minimal dose of  $5 \times 10^6$  AdBMP2-transduced cells. This number of cells yields approximately 93 ng of total BMP2 protein within culture supernatant over a 5-day period. Although lesser numbers of AdBMP2-transduced cells ( $5 \times 10^5$ ) or BMP2 (9 ng) did result in heterotopic bone formation, it was not enough to reliably heal the fibula defect. Smaller doses, such as 1 ng, were unable to induce HO. Delivery of additional cells beyond  $5 \times 10^6$  resulted in a similar volume of bone, suggesting that there is an upper threshold at which BMP2 receptors are saturated and no additional response will occur. Further, the volume of bone obtained when  $5 \times 10^6$  AdBMP2-transduced cells were delivered to the defect was larger than required for complete healing, and substantial resorption was observed within the first 2–4 weeks as the fibula regained its physiological shape.

Interestingly, recombinant BMP2 studies in rat shows that minimal bone formation is detected at protein levels less than 10  $\mu\text{g}$  [Vogelin et al., 2005], which is 130 times more BMP2 than we require for complete healing (Figs. 2 and 3). This indicates that the BMP2 protein produced by the adenovirus-transduced cells is likely more active or potent than the purified recombinant protein. In addition, this concentration is roughly in the range of physiological concentrations of BMP2, revealing that this system is very unique and perhaps should not be compared to systems employing the recombinant protein [Sciadini and Johnson, 2000; Vogelin et al., 2000, 2005]. The ability to generate, in vivo, biologically active BMP2 in the physiological range similar to what would be expected during bone fracture [Kloen et al., 2002, 2003; Kugimiya et al., 2005] or reduction of blood flow [Yao et al., 2010] suggests that the BMP2 produced in vivo in the eukaryotic cells may be mimicking physiological scenarios that lead to repair of fractures.

The kinetics of bone healing appears to be similar to fracture callus, with a large disorganized structure within the defect area initially formed and successive remodeling and resorption to produce a structure similar to the original fibula. The initial new bone was observed within 10 days of delivery, with the first emergence of a remodeled bone with cortical appearance and inner marrow cavity appearing at 6 weeks. However, approximately half of the samples at 6 weeks still had one cortical bone interface that did not appear contiguously remodeled yet (Fig. 4H), suggesting that the bone had not completely remodeled yet. However, at 9 weeks, all samples appeared to be well remodeled with visible contiguous cortical bone, suggesting that at this point all defects were reliably healed. We observed little change from 9 to 12 weeks; although there was additional bone observed associated with the newly formed skeletal bone. The majority of the bone remodeling and resorption occurred within the first 4 weeks, where the callus-like structure resorbs and begins to form bone in the shape of the original fibula.

Histological analysis of the bone healing within the defect supports the subsequent findings. A large amount of mature bone and cartilage that extend away from the defect site are observed at 2 weeks (Fig. 5A). By 6 weeks and beyond, the bone was more restricted to the defect region (Fig. 5C–E). Although substantial immature woven bone was observed at 4 weeks, by 6 weeks remodeled bone with defined cortical structures could be seen (Fig. 5B,C), suggesting that substantial remodeling and maturation was occurring between 4 and 6 weeks. Again little change occurs histologically between 9 and 12 weeks, suggesting that the bone was maintained and healing was complete. Interestingly, in these tissues the cortical bone appeared to be contiguous. Since the exact shape of the original fibula was not achieved, this may suggest that the signals which would direct and define the exterior cortices may be lacking in this model.

In conclusion, bone healing of a critical size defect in the rat fibula could be rapidly achieved through injection of a cell-based gene therapy system. This system delivered 130 times less BMP2 protein compared to studies using recombinant protein as the osteoinductive agent and was able to induce bone within a physiological range of BMP2 concentration. Thus, this cell-based approach is reliable, efficacious, and importantly has additional

safety in that no free virus or infectious agents of any kind would be delivered to patients. These studies are the first step in developing a cell-based gene therapy which effectively harnesses the capacity of BMP2 to generate bone at target locations and rapidly repair skeletal bone.

## ACKNOWLEDGMENTS

This work was supported in part by grants from Department of Defense (DAMD) W81XWH-07-1-0215 and Defense Advanced Research Agency (DARPA) W911NF-09-1-0040 (to E.A.O).

## REFERENCES

- Baltzer AW, Lattermann C, Whalen JD, Ghivizzani S, Wooley P, Krauspe R, Robbins PD, Evans CH. 2000. Potential role of direct adenoviral gene transfer in enhancing fracture repair. *Clin Orthop Relat Res* (379 Suppl):S120–S125.
- Blum JS, Li RH, Mikos AG, Barry MA. 2001. An optimized method for the chemiluminescent detection of alkaline phosphatase levels during osteodifferentiation by bone morphogenetic protein 2. *J Cell Biochem* 80:532–537.
- DeCoster TA, Simpson AH, Wood M, Li G, Kenwright J. 1999. Biologic model of bone transport distraction osteogenesis and vascular response. *J Orthop Res* 17:238–245.
- DeCoster TA, Gehlert RJ, Mikola EA, Pirela-Cruz MA. 2004. Management of posttraumatic segmental bone defects. *J Am Acad Orthop Surg* 12:28–38.
- Endo M, Kuroda S, Kondo H, Maruoka Y, Ohya K, Kasugai S. 2006. Bone regeneration by modified gene-activated matrix: Effectiveness in segmental tibial defects in rats. *Tissue Eng* 12:489–497.
- Finkemeier CG. 2002. Bone-grafting and bone-graft substitutes. *J Bone Joint Surg Am* 84-A:454–464.
- Fouletier-Dilling CM, Gannon FH, Olmsted-Davis EA, Lazard Z, Heggeness MH, Shafer JA, Hipp JA, Davis AR. 2007. Efficient and rapid osteoinduction in an immune-competent host. *Hum Gene Ther* 18:733–745.
- Gafni Y, Pelled G, Zilberman Y, Turgeman G, Apparailly F, Yotvat H, Galun E, Gazit Z, Jorgensen C, Gazit D. 2004. Gene therapy platform for bone regeneration using an exogenously regulated, AAV-2-based gene expression system. *Mol Ther* 9:587–595.
- Gelse K, Jiang QJ, Aigner T, Ritter T, Wagner K, Poschl E, von der Mark K, Schneider H. 2001. Fibroblast-mediated delivery of growth factor complementary DNA into mouse joints induces chondrogenesis but avoids the disadvantages of direct viral gene transfer. *Arthritis Rheum* 44:1943–1953.
- Giannoudis PV, Atkins R. 2007. Management of long-bone non-unions. *Injury* 38(Suppl 2):S1–S2.
- Gugala Z, Olmsted-Davis EA, Gannon FH, Lindsey RW, Davis AR. 2003. Osteoinduction by ex vivo adenovirus-mediated BMP2 delivery is independent of cell type. *Gene Ther* 10:1289–1296.
- Haidar ZS, Hamdy RC, Tabrizian M. 2009. Delivery of recombinant bone morphogenetic proteins for bone regeneration and repair. Part B: Delivery systems for BMPs in orthopaedic and craniofacial tissue engineering. *Bio-technol Lett* 31:1825–1835.
- Hollinger JO, Schmitt JM, Buck DC, Shannon R, Joh SP, Zegzula HD, Wozney J. 1998. Recombinant human bone morphogenetic protein-2 and collagen for bone regeneration. *J Biomed Mater Res* 43:356–364.
- Jeon O, Song SJ, Kang SW, Putnam AJ, Kim BS. 2007. Enhancement of ectopic bone formation by bone morphogenetic protein-2 released from a heparin-conjugated poly(L-lactic-co-glycolic acid) scaffold. *Biomaterials* 28:2763–2771.
- Kloen P, Doty SB, Gordon E, Rubel IF, Goumans MJ, Helfet DL. 2002. Expression and activation of the BMP-signaling components in human fracture nonunions. *J Bone Joint Surg Am* 84-A:1909–1918.

- Kloen P, Di Paola M, Borens O, Richmond J, Perino G, Helfet DL, Goumans MJ. 2003. BMP signaling components are expressed in human fracture callus. *Bone* 33:362–371.
- Kugimiya F, Kawaguchi H, Kamekura S, Chikuda H, Ohba S, Yano F, Ogata N, Katagiri T, Harada Y, Azuma Y, Nakamura K, Chung UI. 2005. Involvement of endogenous bone morphogenetic protein (BMP) 2 and BMP6 in bone formation. *J Biol Chem* 280:35704–35712.
- Laurencin C, Khan Y, El-Amin SF. 2006. Bone graft substitutes. *Expert Rev Med Devices* 3:49–57.
- Lieberman JR, Le LQ, Wu L, Finerman GA, Berk A, Witte ON, Stevenson S. 1998. Regional gene therapy with a BMP-2-producing murine stromal cell line induces heterotopic and orthotopic bone formation in rodents. *J Orthop Res* 16:330–339.
- Motsitsi NS. 2008. Management of infected nonunion of long bones: The last decade (1996–2006). *Injury* 39:155–160.
- Moutsatsos IK, Turgeman G, Zhou S, Kurkalli BG, Pelled G, Tzur L, Kelley P, Stumm N, Mi S, Muller R, Zilberman Y, Gazit D. 2001. Exogenously regulated stem cell-mediated gene therapy for bone regeneration. *Mol Ther* 3:449–461.
- Olmsted EA, Blum JS, Rill D, Yotnda P, Gugala Z, Lindsey RW, Davis AR. 2001. Adenovirus-mediated BMP2 expression in human bone marrow stromal cells. *J Cell Biochem* 82:11–21.
- Olmsted-Davis EA, Gugala Z, Gannon FH, Yotnda P, McAlhany RE, Lindsey RW, Davis AR. 2002. Use of a chimeric adenovirus vector enhances BMP2 production and bone formation. *Hum Gene Ther* 13:1337–1347.
- Sciadini MF, Johnson KD. 2000. Evaluation of recombinant human bone morphogenetic protein-2 as a bone-graft substitute in a canine segmental defect model. *J Orthop Res* 18:289–302.
- Sen MK, Miclau T. 2007. Autologous iliac crest bone graft: Should it still be the gold standard for treating nonunions? *Injury* 38(Suppl 1):S75–S80.
- Sorger JJ, Hornicek FJ, Zavatta M, Menzner JP, Gebhardt MC, Tomford WW, Mankin HJ. 2001. Allograft fractures revisited. *Clin Orthop Relat Res* (382):66–74.
- Thies RS, Bauduy M, Ashton BA, Kurtzberg L, Wozney JM, Rosen V. 1992. Recombinant human bone morphogenetic protein-2 induces osteoblastic differentiation in W-20-17 stromal cells. *Endocrinology* 130:1318–1324.
- Tzioupis C, Giannoudis PV. 2007. Prevalence of long-bone non-unions. *Injury* 38(Suppl 2):S3–S9.
- Vogelin E, Brekke JH, Jones NF. 2000. Heterotopic and orthotopic bone formation with a vascularized periosteal flap, a matrix and rh-BMP-2 (bone morphogenetic protein) in the rat model. *Mund Kiefer Gesichtschir* 4(Suppl 2):S454–S458.
- Vogelin E, Jones NF, Huang JI, Brekke JH, Lieberman JR. 2005. Healing of a critical-sized defect in the rat femur with use of a vascularized periosteal flap, a biodegradable matrix, and bone morphogenetic protein. *J Bone Joint Surg Am* 87:1323–1331.
- Vyrostek SB, Annett JL, Ryan GW. 2004. Surveillance for fatal and nonfatal injuries—United States, 2001. *MMWR Surveill Summ* 53:1–57.
- Watson JT, Anders M, Moed BR. 1995. Management strategies for bone loss in tibial shaft fractures. *Clin Orthop Relat Res* (315):138–152.
- Winn SR, Hu Y, Sfeir C, Hollinger JO. 2000. Gene therapy approaches for modulating bone regeneration. *Adv Drug Deliv Rev* 42:121–138.
- Yao Y, Bennett BJ, Wang X, Rosenfeld ME, Giachelli C, Lusis AJ, Bostrom KI. 2010. Inhibition of bone morphogenetic proteins protects against atherosclerosis and vascular calcification. *Circ Res* 107:485–494.